Advanced Journal of Engineering and Scientific Applications (AJESA)

Research Paper Open Access

Available online at www.ajesa.com.ng

Vol.1, No.1, 2024. pp.16-28



Effect of ceramic filler materials on abrasive wear performance of glass/epoxy composites

George O. Okoronkwo¹, Chidobere David Nwa-David²

¹Department of Chemical Engineering, Micheal Okpara University of Agriculture, Umudike, Abia State, Nigeria; okoronkwo.george@mouau.edu.ng, ogeorgeonyeka@gmail.com

Corresponding Author:ogeorgeonyeka@gmail.com

Abstract

When creating polymer-based composites, plain weave fabrics and micron-sized fillers offer bidirectional strength and reduced voids/inhomogeneity. The aim of the present investigations, is effect of ceramic filler materials on abrasive wear performance of Glass/Epoxy Composites. These were studied during three body abrasive wear with and without ceramic fillers (, , graphite, and fly ash cenospheres). In experiments, loads of 20 N and 40 N were applied at various abrading distances of 500 m, 1000 m, 1500 m, and 2000 m. According to the results of sand abrasive wear test, the specific wear rates of G-E based composites are sensitive to fibre and filler/matrix adhesion. Under all tribo-test settings, the SWR for all particulate G-E composites decreases in the following order: G-E > Gr/G-E > /G-E > fly ash cenosphere/G-E. Furthermore, the specific wear rate of the fly ash cenosphere filled G-E composites was found to be lower than the G-E and other filler materials filled G-E composites. There was 38.7% reduction in the specific wear rate at 40 N, 2000 m in fly ash cenosphere filled G-E composite. As per the evidence of scanning electron microscope images of worn-out surfaces, mechanisms such as ploughing, fibre breakage, fibre pull-out, fibre thinning, and a network of micro-cracks caused the wear in composites

KEYWORDS: Bidirectional glass-epoxy composites; Ceramic fillers; Three-body abrasive wear; Wear volume; Specific wear rate

1. INTRODUCTION

A recent study found that glass fibers have been used as strengthening agent with epoxy matrix material for structural applications (Megahed et al. 2018). Some advantages include high specific characteristics, low cost, bidirectional strength, and simplicity of handling. They are employed in the building and automotive industries due to its superior mechanical qualities, low cost, and ease of fabrication (Nayak et al. 2019). Gears, bearings, and sleeves are just a few examples of mechanical components that frequently make use of polymers and their mono and hybrid composites. This is a prominent class of man-made composite materials for tribo-engineering, where tribo-performance in non-lubricated settings is a key material selection characteristic (Darshan et al. 2022). Fiber and particulate-reinforced epoxy composite materials have suitable tribological characteristics ((Kiran et al. 2018), (Negawo et al. 2021), (Gafsi et al. 2021; Dass et al. 2017). The number of research articles on epoxy as a matrix material with glass fibres and ceramic fillers for improving the qualities in mechanical and abrasion resistance has increased over the past ten years ((Darshan et al. 2021), (Darshan et al. 2022), (Darshan et al. 2022; Namdev et al. 2022; Darshan et al. 2019; Shivakumar et al. 2019; Muralidhara et al. 2020)). Wind turbine blades were made of polymer composite materials that had glass fibre reinforcement (Darshan et al. 2022).

² Department of Civil Engineering, Micheal Okpara University of Agriculture, Umudike, Abia State, Nigeria nwadavid.chidobere@mouau.edu.ng, nwadavid.chidobere@mouau.edu.ng

Table 1: Summary of the wear behaviour of micron sized particulates reinforced composites.

Table 1: Summary of the wear be			
Composite	Fabrication	Loading of filler	Output
MoS2 and Al2O3 fillers	Hand lay-up	5, and 10 wt. %	Inclusion of MoS2 and Al2O3
+ CF-epoxy		each	composites separately improved the
			two-body abrasive wear resistance.
Graphite and alumina	Hand lay-up	2.5, 5 and 7.5 wt. %	Alumina filled GF-epoxy composite
+ GF-epoxy			enhanced the wear resistance, while
			graphite filler worsens the wear
			resistance of the GF-epoxy
Cenospheres +Polyester	Open mould	10 wt.%	Submicron size cenospheres
	casting		decreased the CoF and specific wear
			rate.
Cenospheres + vinyl ester	Open mould	10 wt.%	Submicron size cenospheres
	casting		contributed to increase in the wear
			resistance
SiC, Al2O3, and ZnO particulates	Open mould	10 wt. % each	All micron size fillers show
+novolac epoxy	casting		improved wear resistance and
			reduced CoF.
Graphite + epoxy	Open mould	10 wt.% (20 μ)	5 wt. % graphite reduced the CoF
	casting	5 wt. % -(10 μ)	and enhanced the wear resistance.
Nano-Al2O3 +chopped carbon	Open mould	1, 2, 4 and 6 wt. %	CFs are very effective in reducing
fiber + epoxy	casting	CF	CoF
		4 wt.% CF + 1, 2, 3	Specific wear rate decreased by
		and	releasing a quantity of lubricant film
		4 wt. % Nano-	on the counterface.
N. 41000 8100	0 11	Al2O3	
Nano-Al2O3, nano-SiO2, nano-	Open mould	1, 2, 3 and 4 wt. %	Addition of 3 wt.% of silane treated
zirconia, gypsum micro-filler	casting	each	nano-silica in the dental composite
+Monomer resin BisGMA			evidenced effective for enhancing
N C'02 1 1 1 1 1	77 ' C '	0.1.0.5. 1.0.0	the wear resistance.
Nano-SiO2 and carbon nanotubes	Vacuum infusion	0.1, 0.5 and 0.9	Both nano-particles improved
+ carbon-epoxy	process	wt. % each	friction coefficient and wear rates of
C1	TT 11	10 4 50 4 0/	carbon-epoxy
Glass fiber + epoxy	Hand lay-up	10 to 50 wt. %	Short GF-epoxy composites were
		Short GF	found to exhibit higher wear
		10 to 50 wt. %	resistance than that of the
F 1 C1 : 1 :4	TT 11	Woven GF	bidirectional GF-epoxy composites
E-glass fabric+ epoxy composites	Hand lay-up	2.5, 5 and 7.5 wt. %	Experimental result showed the
with and without graphite filler			following trend for abrasive wear
			rate: graphite filled GF-epoxy
SiC montioulate + CE	Hand 1	2.5.5 and 7.5 + 0/	composites>GF-epoxy
SiC particulate + GF-epoxy	Hand lay-up	2.5, 5 and 7.5 wt. %	Experimental results showed the
			positive impact of SiC fillers, which
			enhanced the abrasive wear
			resistance of GF-epoxy composites

Several research looked at the use of micron-sized fillers to improve the abrasion resistance of polymer composites reinforced with glass fibre materials ((Kiran et al. 2018), (Negawo et al. 2021), (Gafsi et al. 2021; Dass et al. 2017; Kumar et al. 2018)). According to research by Hemanth et al., the specific wear rate of TCE + PTFE composite composites is high, but it can be decreased by adding micron-sized fillers (silicon carbide, pine bark dust) to the TCE + PTFE composite (Manjunath et al. 2016). (Sharma et al. 2020) investigated whether adding fly ash improved the abrasion resistance of epoxy composites bonded with glass fibre. (Ibrahem et al. 2016) investigated the three-body abrasive wear behaviour of epoxy composites reinforced with carbon fabric. They found that incorporating micron-sized SiC particles into the same increasesits resistance to abrasion. The effects of TiO2 and ZnO on the use of bidirectional glass reinforced polyester composites were examined by (Ibrahem et al. 2016). -filled hybrid composites outperformed ZnO-filled hybrid composites in testing, the researchers found. The thermo-mechanical and wear characteristics of woven glass fibre composites that have silicon carbide incorporated were studied by (Suresha et al. 2021). The results showed a rising or falling trend as well as important components in each analysis. There was also discussion of the trend and key factors affecting the decrease in specific wear rate. Most recent literatures ((Kiran et al. 2018), (Negawo et al. 2021), (Gafsi et al. 2021; Dass et al. 2017; Kumar et al. 2018; Ayatollahi et al. 2019; Qian et al.



© 2025. Advanced Journal of Engineering and Scientific Applications (AJESA) Vol. 2, No..1, 2025.

2019)) on micro and nano sized fillers are provided in Table 1. Hence, this study aimed to illustrate how different micron-sized fillers, including silicon dioxide, alumina, graphite, and fly ash cenosphere particulates, affected the behaviour of three-bodies of abrasive wear, in particular the specific wear rate of bidirectional glass fabric reinforced epoxy composites. For different abrading distances with a constant applied load and rubber wheel speed, the wear volume as well as specific wear rate was computed.

Natural fibre composites are biodegradable and are low cost than synthetic fibre composites. These natural fibres are easily available and best suited for manufacturing, making some researchers focus on reinforcements specifications for better-reinforced polymer composite (Miyoshi et al. 2019). Over the past few years, till now researchers are performed to substitute synthetic with natural fibers. These natural fibres have better qualities like high specific mechanical properties, renewable and biodegradable with low cost (Ibrahem et al. 2016). These natural fiber-reinforced polymer composites have better tri-biological properties than synthetic fibre material (Ibrahem et al. 2016). Even industrial applications like bearings, flooring materials, and brake pads require friction coefficient and Wear resistance (Ibrahem et al. 2015). The demand for polymer composite reinforced natural fibres has attained attention as these have excellent environmental properties, which are affordable and easy to manufacture than synthetic fibres ((Shalwan et al. 2021), (Ibrahem et al. 2015)). Due to these excellent properties, polymer composites are used in the construction, automobile and furniture industries (Zagho et al. 2018).

These natural polymer composites are distinguished by their unique low density and cost properties, flexible processing equipment, and best mechanical properties with high strength, chemically resistant than synthetic fibres ((Alajmi et al. 2022), (Darshan et al. 2021)). For a polymer composite matrix, a better option than synthetic fibre would be natural fibres like sisal, coir, date palm corn, and silk for better reinforcement polymer composite in the current situation (Darshan et al. 2022). There is an increase in research on natural fiber-reinforced composites in both mechanical and tri-biological applications. ((Darshan et al. 2022), (Namdev et al. 2022) and (Vinod et al. 2018)). These natural fiber-reinforced composite polymers can enhance their performance in tensile, impact, Wear, flexural, friction and other mechanical and tri-biological applications ((Darshan et al. 2016), (Namdev et al. 2023) and (Namdev et al. 2022)).

Research is being carried out on the effect of fibre materials, additives and their further modifications, and their content percentages on polymer composites' mechanical and tri-biological properties (Yan et al. 2020). There is still a debate between many scholars' research on the relationship between mechanical and tri-biological performances of material ((Chira et al. 2016), (Namdev et al. 2021) and (Shivakumar et al. 2020)). However, carbon has specific selective effects on mechanical performance, while frictional properties are more favourable (Srivastava et al. 2019). (Kumar et al. 2020) Investigated coir epoxy composite with various ratios and stated that the wear resistance of coir fibre mainly focuses on their dust particle size and normal load applied. He also stated that the wear mechanism had been dominated by reinforcement due to high coir dust loading (Kumar et al. 2020).

These natural fibre composites had many desirable properties, like yielding low-density material relative to composite properties. These are low in cost, and processing has also been a renewable resource. had researched rice husk-reinforced epoxy composite and found better results on abrasive wear loss by suitable treatment ((Scedil et al. 2019) and (Muralidhara et al. 2020)). Palm and mangos dry leaves also improve tri biological properties of polymer composites ((Darshan et al. 2019) and (Tahir et al. 2016)).

Our work proposes coir and sisal fibres with reinforced polymer composites to improve their wear and friction behaviour for proposed composite materials. Three orientations, parallel, anti-parallel and normal, are tested for polymeric composite under different loads from 5 to 60 N and are applied through Various Grade papers and Time Intervals to find the abrasiveness of developed composites

2. MATERIALS AND METHODS

2.1 Materials

Used materials are plain weave woven glass fibres weighing 360 g/m² (E-glass) with fibre diameters ranging from 10 to 13 μ m. LAPOX L12 epoxy resin and K-6 hardener in a 100:12 weight ratio. Both materials were purchased by Nycil CCRD Limited, Nigeria. Micron sized ceramic particles namely SiO₂, Al₂O₃, graphite (Gr), and fly ash cenosphere were collected from commercially available sources and used without further treatment. The average particle sizes of Al₂O₃, graphite, fly ash cenosphere and silica were 20 μ m, 25 μ m and 25 μ m respectively. The hand lay-up method was used to create G-E composite laminates (200 mm \times 200 mm \times 10 mm) with and without ceramic fillers as listed in Table 2, which were then vacuum-bagged.

• Initially number of glass fibre layers required (55 wt. %) to achieve laminate thickness of 10 mm were cut for the



© 2025. Advanced Journal of Engineering and Scientific Applications (AJESA) Vol. 2, No..1, 2025.

dimension of 200 mm \times 200 mm.

- Epoxy matrix along with hardener (35 wt. %) and micro sized fillers were mixed together thoroughly.
- First layer of the glass fibre was placed on the flat surface pre-cleaned with acetone.
- Epoxy mixture was then coated over the first layer with the help of a hand brush and thereafter second layer of the fabric was placed on the first layer.
- This process of applying the epoxy mixture and placing of new glass fibre layer was continued till desired thickness of 10 mm was measured.
- Air trapped between the layers of glass fibres were removed by placing the fabricated laminate in vacuum bag for 90 minutes duration.
- This was followed by curing the laminates at 120 °C for 120 min.

Table 2: Composite materials designations

Composites	Alumina (wt.%)	Fly ash (wt.%)	Graphite (wt.%)	Silica (wt.%)
G-E	-	-	=	=
Alumina G-E	10	-	-	-
Fly ash G-E	-	10	-	-
Graphite G-E	-	-	10	-
Silica G-E	-	-	-	10

Table 3: Water jet machining parameters

Parameter	Magnitude
Water pressure	200 MPa
Abrasive flow rate	300 g/min
Transverse speed	125 mm/min
Stand-off distance	1.5 mm

Laminates were then cut into the size of 75 mm x 25 mm x 10 mm for abrasion test with the help of water jet machining using cutting parameters provided in Table 3. 2.1 Three-body abrasion test A diagrammatic representation of a Rubber wheel test rig is shown in Figure 1 and its specifications are provided in Table 4. The test samples are first weighed with a weighing balance machine (Make: Sartorius BSA224S-CW, Least Count: 0.0001 g) and their initial mass were noted (mi).

Table 4: Specifications of rubber wheel test rig

Parameter	Magnitude
Wheel diameter	228 mm
Rubber wheel thickness	12.7 mm
Wheel speed	200 rpm
Rubber hardness	60 Shore-D
Abrasive sand size	100-200 μm
Abrasive flow rate	350 g/min

The specimen is then put in the test setup's specimen holder, which is located across from the rubber wheel. The loads are then applied. The machine is then run by giving the test samples the required number of rotations, which causes abrasive sand particles to flow clockwise between the rubber wheel and the test sample. At that point, the test sample is being abraded as the wheel rotating at 200 rpm presses up against it and the sand flows downwards via nozzle at the rate of 350 g/min. The machine stops running after the specified number of revolutions, and the test sample is removed from the sample holder and weighed once more (m_f) . This weight is then compared with the sample's initial weight (m_i) , to find the wear mass loss $(\Delta m = m_i - m_f)$ and specific wear rate (SWR, also known as wear factor). The wear tests were conducted with two applied weights (20 N and 40 N), four abrading distances (500 m, 1000 m, 1500 m, and 2000 m), and a constant speed of 200 rpm.

The calculation of the SWR or wear factor (K_s) is done as per ASTM G40 standard using the following equation:

$$K_{s} = \frac{\Delta V}{P \times D} (m^{3}/Nm) \tag{1.0}$$

where, ΔV represents the wear volume loss in m^3 which is obtained by dividing the wear mass loss (Δm in gram) by the density (ρ in g/m^3) of corresponding composite samples i.e. $\Delta V = \Delta m/\rho$ as per ASTM G65; P represents the applied normal load in Newton and D represents the abrading distance in meters. The involved wear mechanisms of the selected abraded test samples were examined using a scanning electron microscope (SEM, Make: JEOL, JSM-IT300 series with magnification of x5-x300000).



© 2025. Advanced Journal of Engineering and Scientific Applications (AJESA) Vol. 2, No..1, 2025.

3. RESULTS AND DISCUSSION

3.1 Effect of filler materials on wear volume

Wear volume loss versus abrading distance for G-E composites filled with various filler materials are shown in Figures 1 and 2 for applied normal loads of 20 N and 40 N, respectively. Compared to metals, polymer composites offer very less resistance to abrasion [40]. Hence, as recommended by ASTM G65 standard, light load variation from 20 N to 40 N was adopted for the conduction of wear tests.

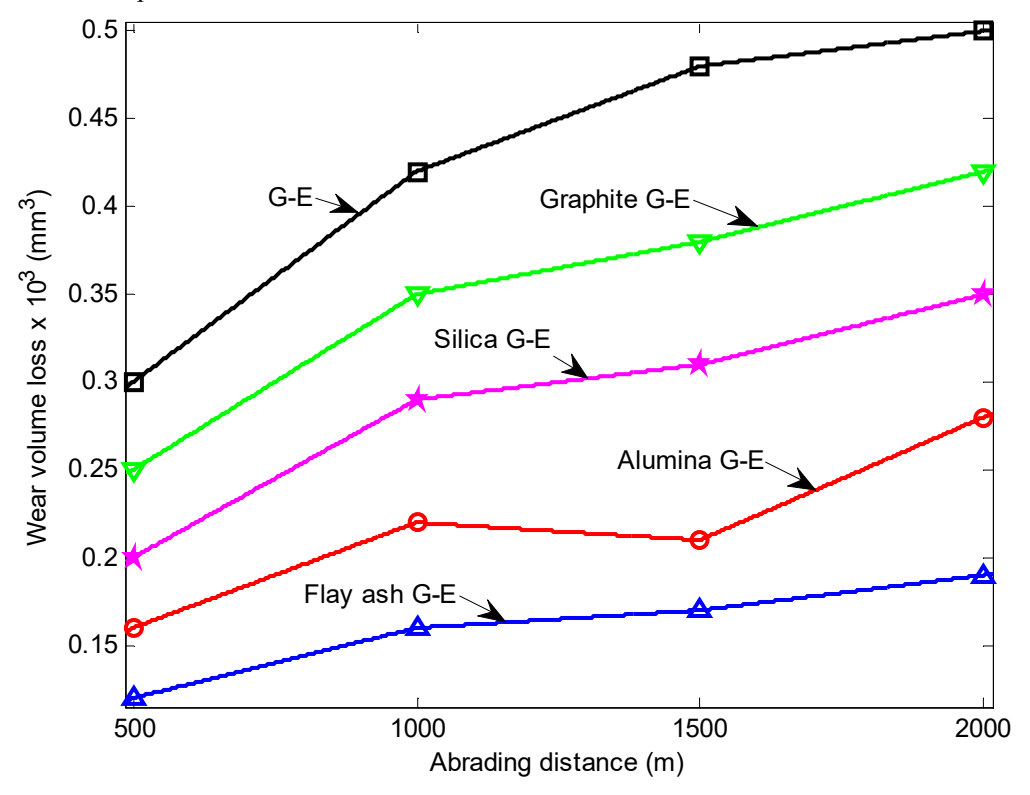


Figure 1: Wear volume loss as a function of abrading distance of filled G-E composites at 20 N.

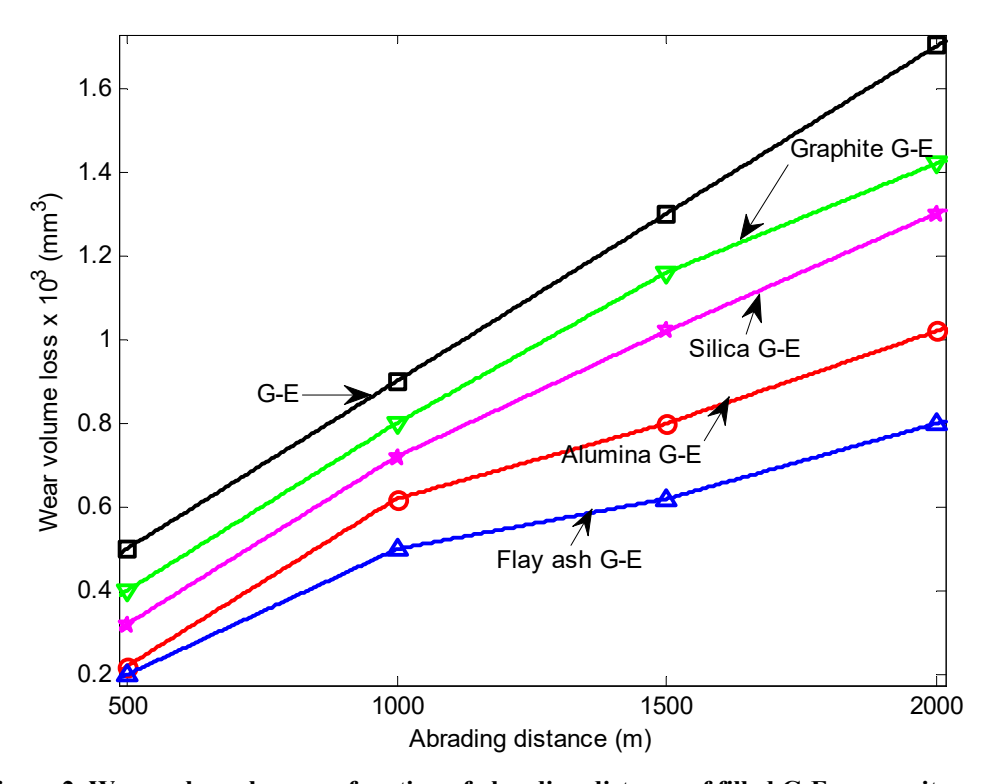


Figure 2. Wear volume loss as a function of abrading distance of filled G-E composites at 40 N



© 2025. Advanced Journal of Engineering and Scientific Applications (AJESA) Vol. 2, No..1, 2025.

In the case of particulate filled G-E composites, fly ash cenosphere filled G-E showed lower wear volume performance. For almost all composite materials, wear volume has shown a saturation level after 1500 m abrading distance. The results in Figures 1 and 2 suggested that the ranking order of the abrasive wear performance of the composite materials changed on the abrading distance and applied normal load. Such variation in the abrasive wear performance depending on the abrading distance has also been reported. Between 500 m and 2000 m of abrading distance were recorded while holding some tribo variables constant (sliding speed: 200 rpm, abrasive size: 225 μm). The figures 2 and 3 demonstrate that with increase in abrading distance, the wear volume steadily increases for all composites having the lowest wear volume loss at the lowest abrading distance of 500 m and the maximum wear volume loss at the highest abrading distance of 2000 m. Among all filled composites, fly ash cenosphere/GE composites had the lowest wear volume loss of 0.128× 103 mm3 at 20 N and 500 m abrading distance, while G-E epoxy composites had the highest wear volume loss. At applied loads of 20 N and 40 N, G-E composite with Al₂O₃ had the second-lowest wear volume loss and SiO₂/G-E composites had the third-lowest wear volume loss as depicted in Figures 1 and 2 respectively.

3.2 Effect of filler materials on specific wear rate

Specific wear rate (SWR) versus abrading distance of G-E and their filler filled G-E composites are depicted in Figures 3 and 4. Figures 3 and 4 show an impact on SWR for Al₂O₃, fly ash cenospheres, SiO₂, and Gr particles filled G-E composites at 20 N and 40 N applied loads, respectively. At 20 N, the SWR gradually decreased as the abrading distance was increased, with the lowest SWR (0.232×10-11 m³N⁻¹m⁻¹) for fly ash filled glass fabric reinforced epoxy composite at the highest abrading distance of 2000 m and the highest SWR (3×10-11 m³N⁻¹m⁻¹ for G-E composite at the smallest abrading distance of 500 m (Figure 4) at 20 N. The SWR of G-E composite varies between 3.386 ×10-11 m³N⁻¹m⁻¹ and 2.113×10-11 m³N⁻¹m⁻¹ with a load application of 40 N and at abrading distances of 500 m and 2000 m, respectively. Fly ash filled G-E composite has SWR values that range from 2.12×10-11 m³N⁻¹m⁻¹ to 1.21×10-11 m³N⁻¹m⁻¹ respectively. Al₂O₃ filled G-E composite has SWR values that range from 2.45×10-11 m³N⁻¹m⁻¹ to 1.43×10-11 m³N⁻¹m⁻¹, respectively.

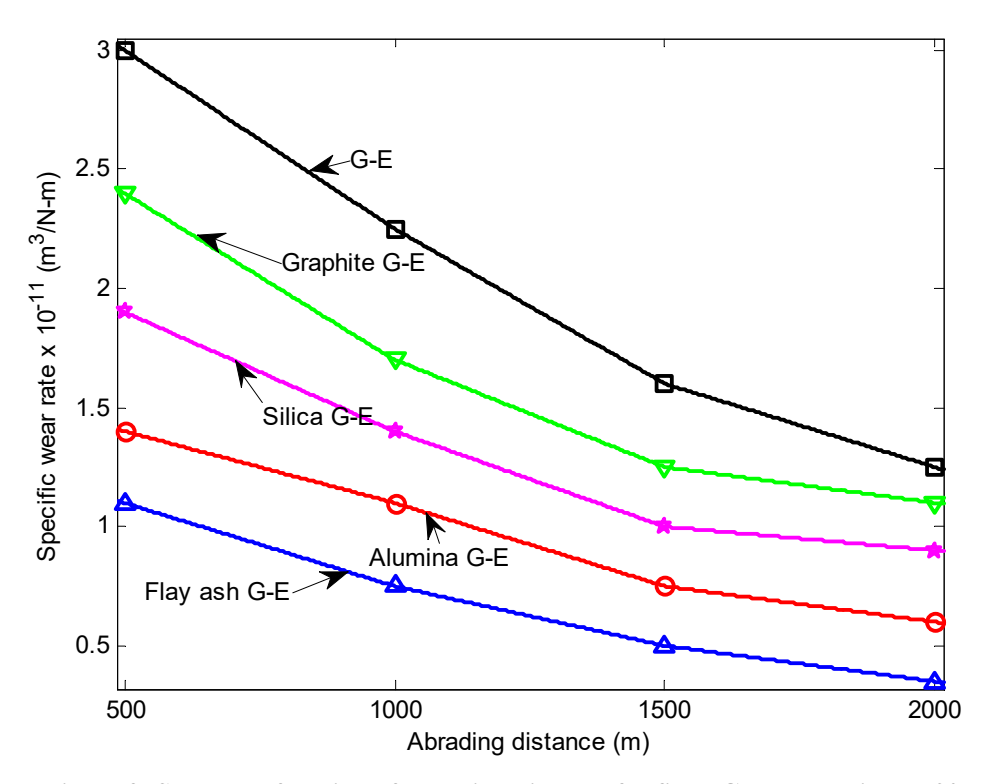


Figure 3: SWR as a function of abrading distance for filled G-E composites at 20N

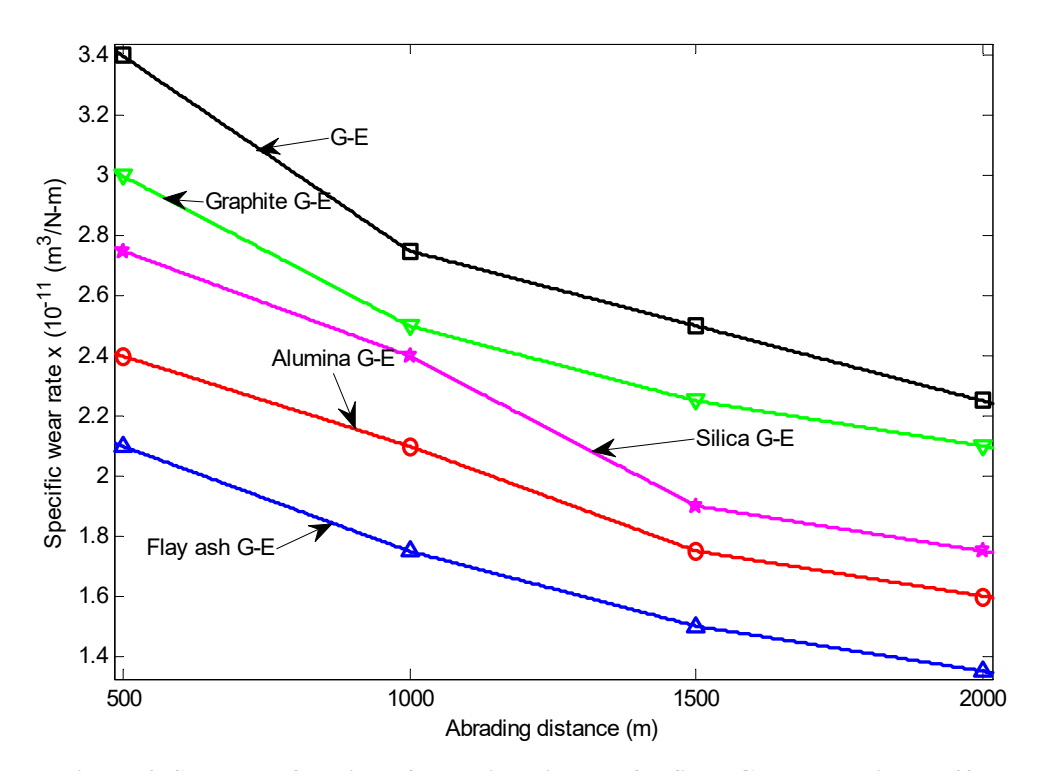


Figure 4: SWR as a function of abrading distance for filled G-E composites at 40 N.

Furthermore, SiO_2/G -E composites have SWR values that range from 2.72×10 -11 m³N⁻¹m⁻¹ to 1.61×10 -11 m³N⁻¹m⁻¹, respectively. Gr filled G-E has SWR values that range from 2.99×10 -11 m³N-1m-1 to 1.88×10 -11 m³N⁻¹m⁻¹, respectively. The applied load of 40 N showed the same trend. Therefore, it can be inferred from the data that the SWR decreases as the abrading distance rises. The maximum SWR for G-E composites has been observed, as illustrated in Figures 6 and 7, when compared to filled G-E composite materials at 500 m abrading distance with 20 N and 40 N applied loads. Fly ash/G-E composite showed the least SWR as compared to other G-E and other filled G-E composites. The SWR in the descending order is as follows: G-E> Gr/G-E> SiO_2/G -E> Al_2O_3/G -E> Fly ash/G-E. When the different filler materials were added to G-E, it appeared better abrasion resistance. Therefore, it may be concluded that the SWR is deceased by the addition of fillers.

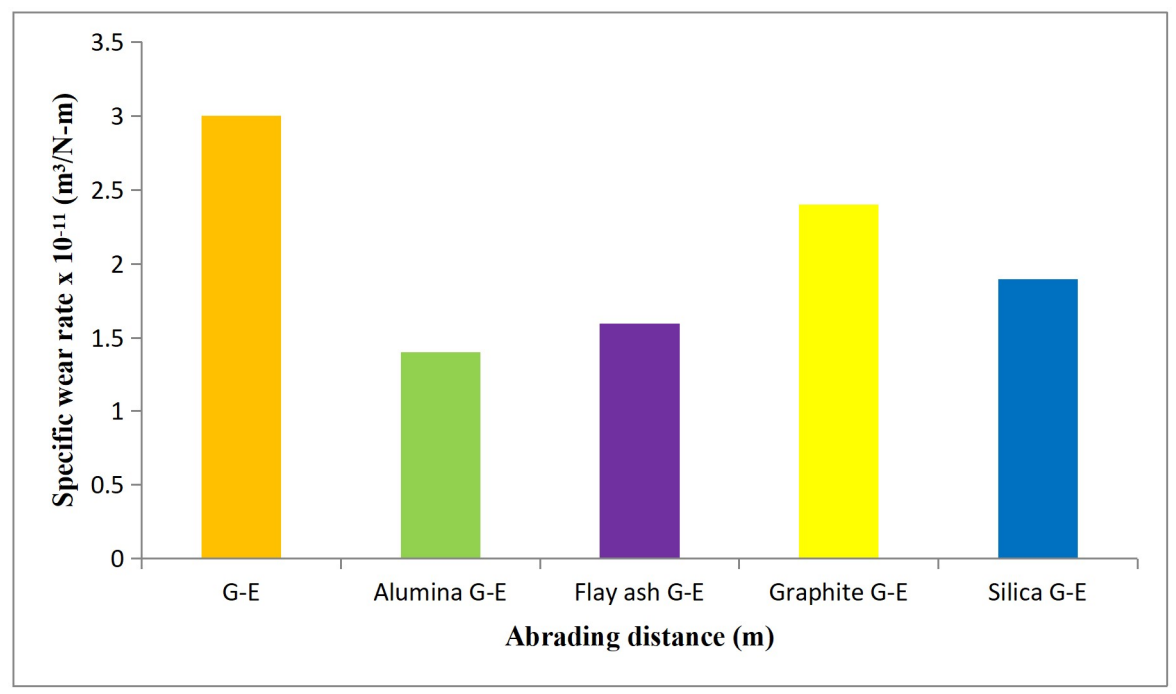


Figure 5: SWR of filled G-E composites at 500m and 20N.



© 2025. Advanced Journal of Engineering and Scientific Applications (AJESA) Vol. 2, No..1, 2025.

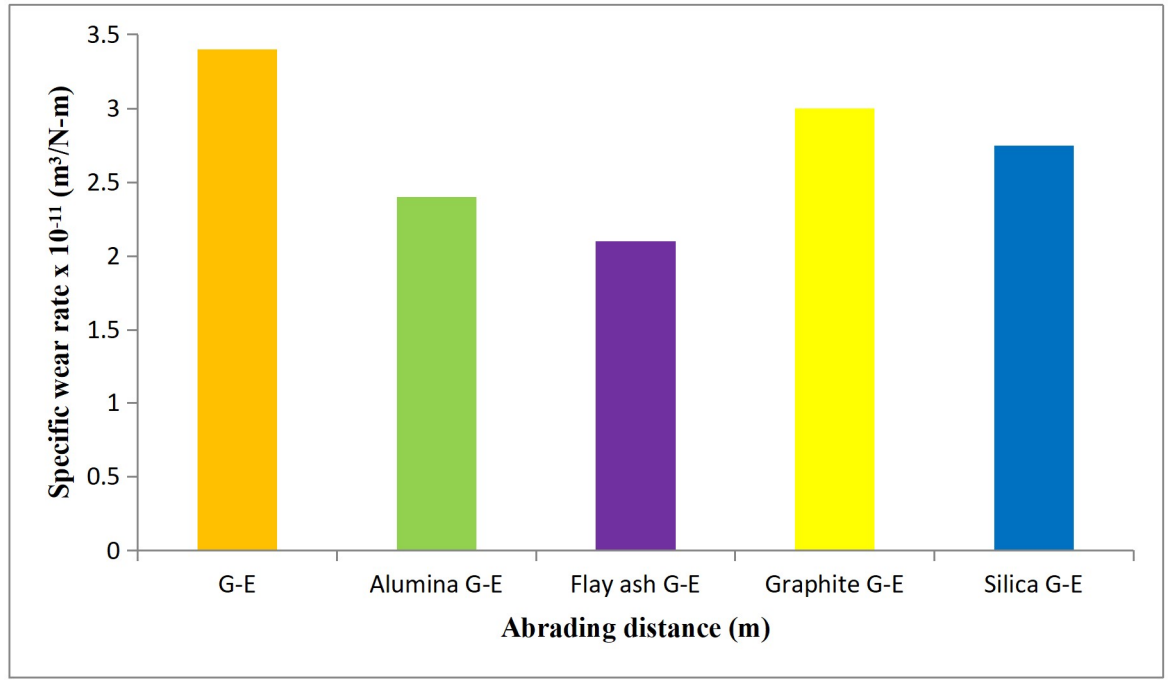


Figure 6: SWR of filled G-E composites at 500m and 40N.

3.3 Internal surface topography of filled G-E composites

Abrasive wear can be affected by several factors like the characteristic motion, surface properties and abrasion properties. Furthermore, abrasion mechanisms can be affected by range of particles size, particle, and surface component properties, contact pressure and velocity of the rubber wheel. The surface deformation depends on the constituents in the final composite. The worn-out composite surfaces were gold sputtered by using the evaporation process with current 15 mA and voltage 1 kV for 10 minutes duration. The gold sputtering process was done to get the conductive coating of 750 Å over the worn surfaces, which is the prerequisite to get good quality SEM images. As illustrated in Figure 8, G-E composite was tested at a normal load application of 40N and a worn surface at 2000 m. Figure 7 demonstrates that under a high applied load (40 N), the damage was more pronounced in the top/bottom resinous regions, with significant fibre degradation in the middle region. It is only possible to discern pitting (denoted by the letter "P") in the resinous areas and a network of micro cracks (denoted by the letter "M") in the vicinity of the bridging glass fibres. Only a few broken fibres were being dragged out, and the clean fibres looked to be intact in the abrading direction with a stepped appearance of glass fibres (marked "SA").

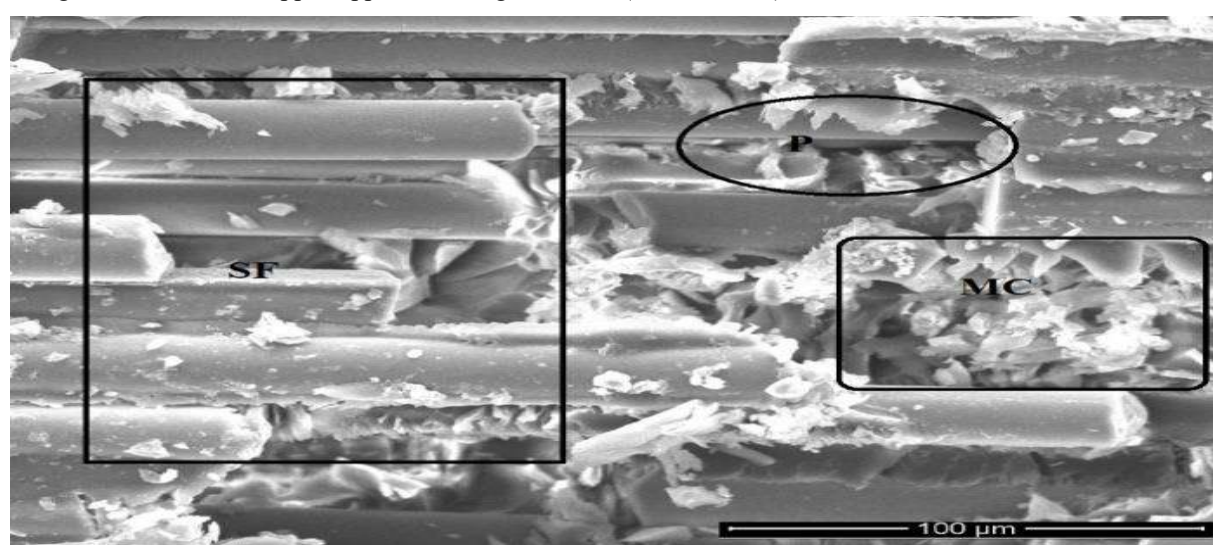


Figure 7: Internal surface topography of G-E composite.

3.4 Internal surface topography of Gr/G-E composites

Figure 9 depicts the wear-out surface of a Gr/GE composite that was tested at a load application of 40 N and 2000 m abrading distance. Figure 8 demonstrates that the epoxy graphite/matrix and fibre areas were both damaged at a high applied load (40 N).



© 2025. Advanced Journal of Engineering and Scientific Applications (AJESA) Vol. 2, No..1, 2025.

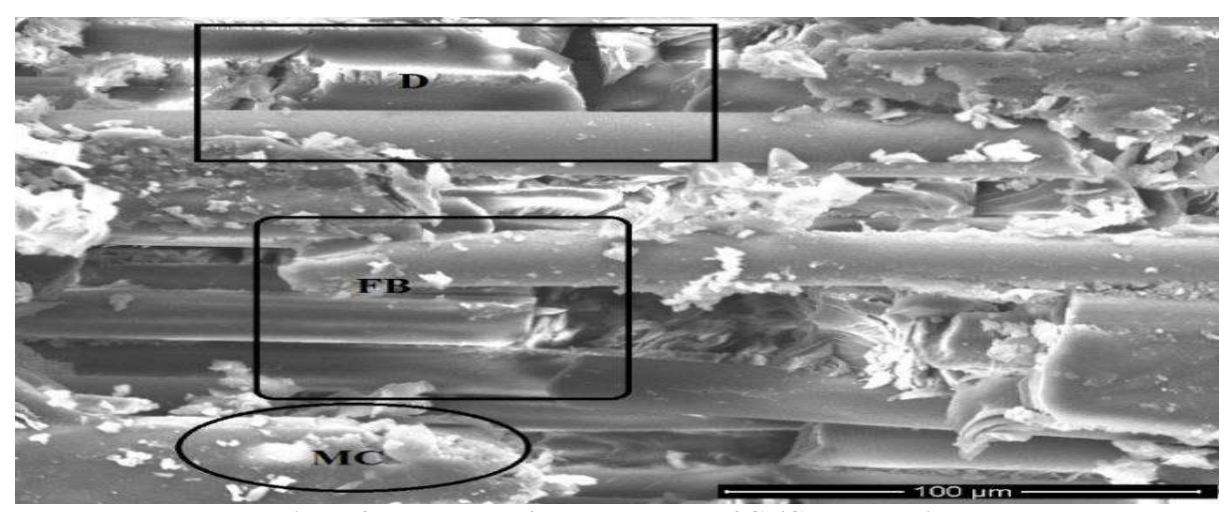


Figure 8; Internal surface topography of Gr/G-E composite.

Delamination (marked "D"), fibre breaking ("FB"), silica sand particles adhered to the epoxy matrix, and micro cracks of epoxy matrix ("MC") all happened. In addition, as shown in Figure 9, breakage occurred in the layered fabric, with broken fibres appearing to be worn-out, and a resinous layer of epoxy matrix with graphite particle pull-out occurred in the matrix/fabric interface region.

3.5 Internal surface topography of SiO₂/G-E composites

Figure 9 depicts the wear-out surface of the SiO_2 / G-E composite that was evaluated at a 40 N load and 2000 m abrading distance. Figure 9's observations of a wear-out surface under higher applied load (40 N) show that the damage was most obvious in the fibrous region, where a large amount of the resinous region near the layers of glass fabrics had been lost. The particles were then encouraged to attack the fibres and cause damage as a result. Additionally, as depicted in Figure 10, the stacked fibers fractured, resulting in the appearance of a steeped layer of broken fibres (designated "SA" in Figure 9) and a resinous layer of epoxy matrix with pull-out of silicon dioxide particles (designated "PO" in Figure 9).

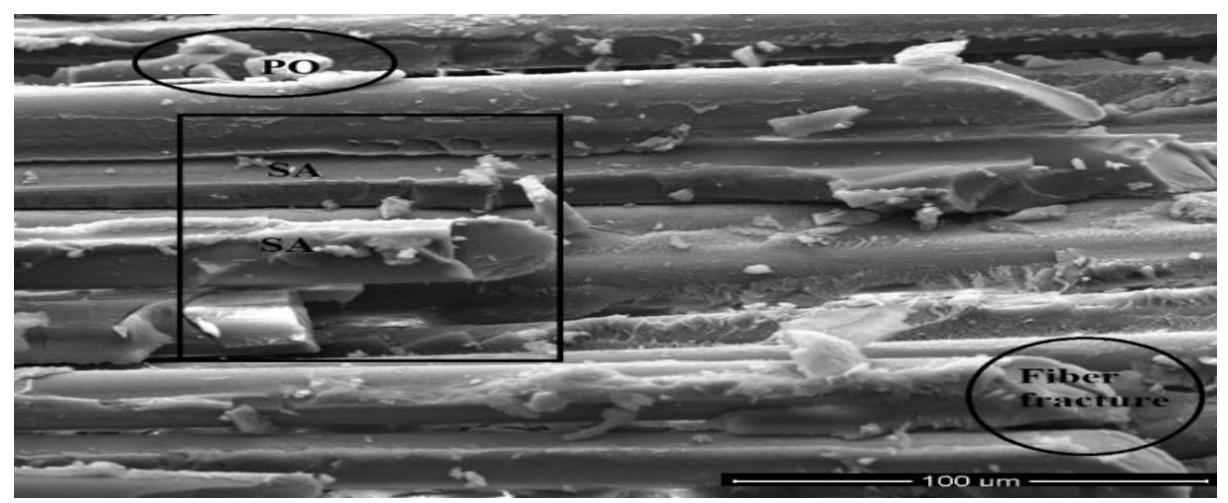


Figure 9: Internal surface topography of SiO₂/G-E composite.

3.6 Internal surface topography of Al₂O₃/G-E composites

The wear behaviour of tribo-materials is sharply affected by the type, shape and size of the ceramic fillers. The presence of ceramic fillers like SiO_2 and Al_2O_3 in G-E composites changed the material surface characteristics by reducing voids and enhancing the structural integrity which resulted in increased abrasion resistance. Figure 10 depicts the wear-out surface of Al_2O_3 filled G-E composite tested at 40N applied normal load and 2000 m. The figure showsconsistent thin resinous layer removal (marked "R") and strong bonding at the interface, which minimizes damage to the epoxy/ Al_2O_3 and glass fibres on the abraded composite surface.

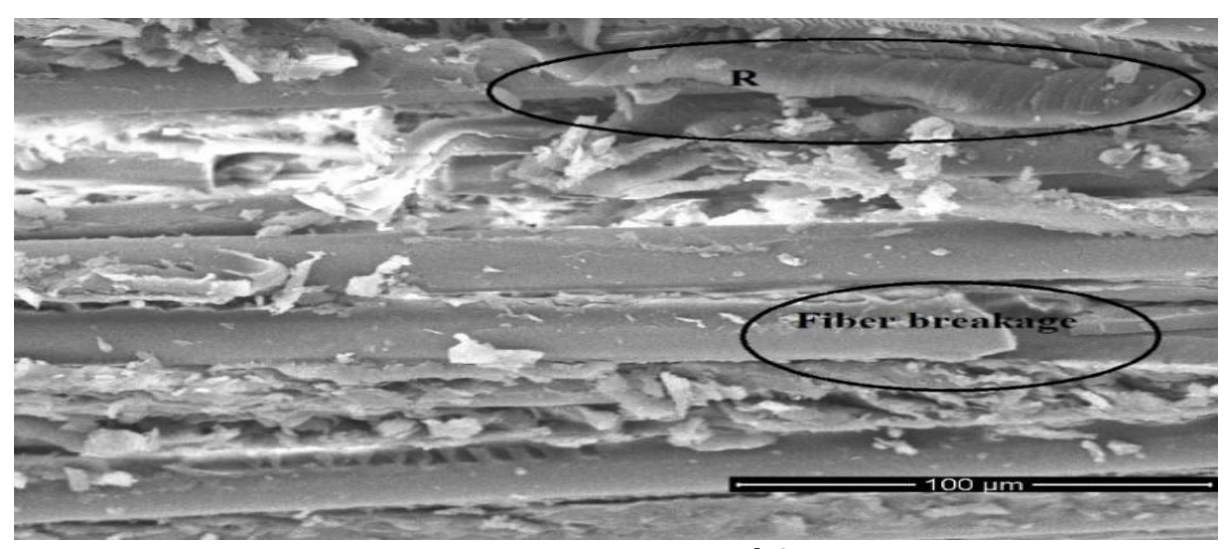


Figure 10: Internal surface topography of Al₂O₃/G-E composite

This indicates that the silica sand fragments were not able to stick to the composite. When comparing the photomicrographs of G-E, Gr/G-E, and SiO₂/G-E composites from Figure 11, it could be inferred that there was only a very small amount of material present that caused less damage to the glass fibres, supporting the wear data.

3.7 Internal surface topography of fly ash/G-E composite

Figure 11 depicts the worn surface of a fly ash filled G-E composite that was tested at a load application of 40N and 2000 m abrading distance. Less damage to the epoxy/fly ash and glass fibres on the abraded composite surface is seen in the image, i.e., uniform thin resinous layer removal (marked "R" in the picture) and strong bonding at the fiber/matrix interface. This indicates that silica sand fragments were not able to stick to composite.

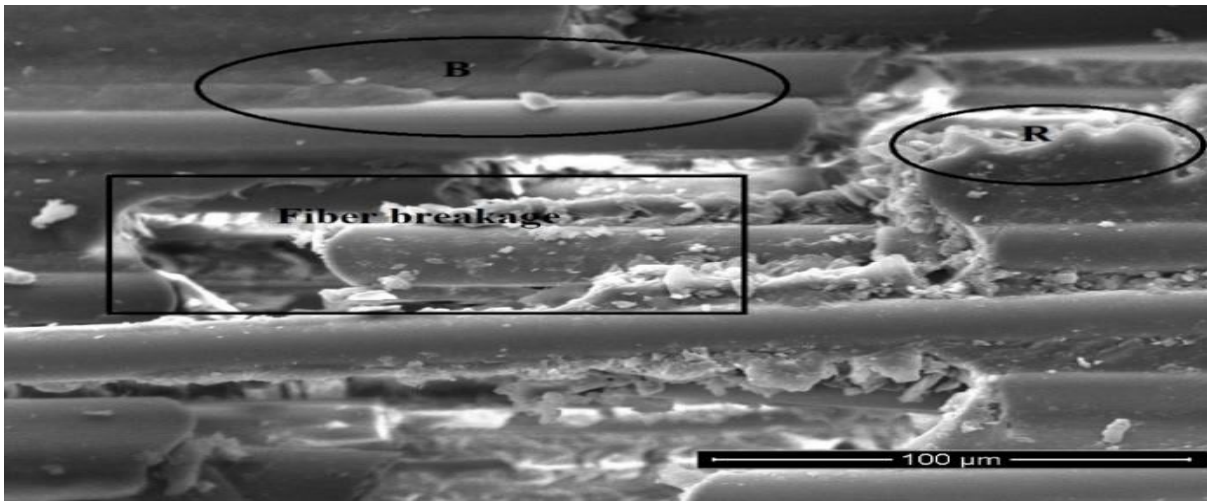


Figure 11: Internal surface topography of Fly ash/G-E composite.

Additionally, larger pieces of epoxy/fly ash particles were discovered on the surface, and the fibres seemed to be fractured but not debonded (indicated as "B"). This was accompanied in some places by little and large cracks, twisted grooves, and pitting. When comparing the photomicrographs of the unfilled Gr, SiO₂ and Al₂O₃ added G-E composites from Figure 12, it is reasonable to infer that there was only a very little amount of material, supporting the least specific wear rate, with less damage to both the matrix/fly ash and glass fibres.

4. CONCLUSION

In this investigation, G-E composites with and without ceramic fillers were made using by hand lay-up method followed by vacuum bagging. Three-body abrasive wear tests produced the following noteworthy results. Incorporation of fly ash cenosphere, , SiO2, and Gr micron-sized fillers into G-E composite revealed good performance in abrasive wear mode. The following factors were observed to be important in controlling the wear performance of the composites. (i) All the fillers (irrespective of shape and size) used in the present work enhanced the epoxy matrix phase's interfacial bonding. (ii) The applied load and abrading distance. (iii) The extent of modification



© 2025. Advanced Journal of Engineering and Scientific Applications (AJESA) Vol. 2, No..1, 2025.

of the composite surface which reduced the wear rate in longer abrading distance run.

Under all trio-test settings, the SWR for all particulate G-E composites decreases in the following order: G-E > G-E >

Photomicrographs show various wear mechanisms of G-E with and without filler. The wear mechanisms involved are ploughing, fibre breakage, fibre pull-out, fibre thinning, and a network of microcracks. The fly ash cenosphere proved to be more wear resistant than, and graphite.

References

- Megahed, A. A., Agwa, M. A., M. Megahed, M. (2018). Improvement of hardness and wear resistance of glass fiber-reinforced epoxy composites by the incorporation of silica/carbon hybrid nanofillers, Polymer-Plastics Technology and Engineering, vol. 57, iss. 4, pp. 251-259, doi: 10.1080/03602559.2017.1320724
- Singh, J., Kumar, M., Kumar, S., S.K. Mohapatra, S. K. (2017). Properties of glass-fiber hybrid composites: a review, Polymer-Plastics Technology and Engineering, vol. 56, iss. 5, pp. 455-469, doi: 10.1080/03602559.2016.1233271
- Nayak, S., Nayak, R. K., Panigrahi, I., A.K. Sahoo, A. K. (2019). Tribo-mechanical responses of glass fiber reinforced polymer hybrid nanocomposites, Materials Today: Proceedings, vol. 18, iss. 7, pp. 4042-4047, doi: 10.1016/j.matpr.2019.07.347
- Kiran, M. D., Govindaraju, H. K., Jayaraju, T. (2018). Evaluation of mechanical properties of glass fiber reinforced epoxy polymer composites with alumina, titanium dioxide and silicon carbide fillers, Materials Today: Proceedings, vol. 5, iss. 10, pp. 22355-22361, doi: 10.1016/j.matpr.2018.06.602
- Negawo, T. A., Polat, Y., Akgul, Y., Kilic, A., M. Jawaid, M. (2021). Mechanical and dynamic mechanical thermal properties of ensete fiber/woven glass fiber fabric hybrid composites, Composite Structures, vol. 259, iss. 1, pp. 113221, doi: 10.1016/j.compstruct.2020.113221
- Manjunath, M., Renukappa, N. M., B. Suresha, B. (2016). Influence of micro and nanofillers on mechanical properties of pultruded unidirectional glass fiber reinforced epoxy composite systems, Journal of Composite Materials, vol. 50, iss. 8, pp. 1109-1121, doi: 10.1177/0021998315588623
- Suresha, B., Divya, G. S., Hemanth, G., Somashekar, H. M. (2021). Physico-mechanical properties of nano silica-filled epoxy-based mono and hybrid composites for structural applications, Silicon, vol. 13, iss. 7, pp. 2319-2335, doi: 10.1007/s12633-020-00812-8
- Kanthraju, B. S., B. Suresha, B. (2016). Enhancement of mechanical properties and wear resistance of epoxy: glass fiber, basalt fiber, polytetrafluoroethylene and graphite, Indian Journal of Advances in Chemical Science S1, pp. 107-113.
- Sharma, V., Meena, M. L., Kumar, M. (2020). Effect of filler percentage on physical and mechanical characteristics of basalt fiber reinforced epoxy-based composites, Materials Today: Proceedings, vol. 26, pp. 2506-2510, doi: 10.1016/j.matpr.2020.02.533
- Singh, A. K., Siddhartha. (2016). Deepak, Assessment of mechanical and three-body abrasive wear peculiarity of TiO2- and ZnO-filled bi-directional E-glass fibre-based polyester composites, Bulletin of Materials Science, vol. 39, pp. 971–988, doi: 10.1007/s12034-016-1237-4
- Gafsi, N., Smaoui, I., Verdejo, R., Kharrat, M., Manchado, M. A., Dammak, M. (2021). Tribological and mechanical characterization of epoxy/graphite composite coatings: Effects of particles' size and oxidation, Proceedings of the Institution of Mechanical Engineers, Part J: Journal of Engineering Tribology, vol. 235, iss. 1, pp. 129-137, doi: 10.1177/1350650120944273
- Dass, K., Chauhan, S. R., Gaur, B. (2017). Study on the effects of nano-aluminium oxide particulates on mechanical and tribological characteristics of chopped carbon fiber reinforced epoxy composites, Proceedings of the Institution of Mechanical Engineers, Part L: Journal of Materials: Design and Applications, vol. 231, iss. 4, pp. 403-422, doi: 10.1177/1464420715598798



© 2025. Advanced Journal of Engineering and Scientific Applications (AJESA) Vol. 2, No..1, 2025.

- Kumar, S. R., Patnaik, A., Bhat, I. K., T. Singh, T. (2018). Optimum selection of nano-and micro sized filler for the best combination of physical, mechanical, and wear properties of dental composites, Proceedings of the Institution of Mechanical Engineers, Part L: Journal of Materials: Design and Applications, vol. 232, iss. 5, pp. 416-428, doi: 10.1177/1464420716629825
- Ayatollahi, M. R., Moghimi Monfared, R., BarbazIsfahani, R. (2019). Experimental investigation on tribological properties of carbon fabric composites: effects of carbon nanotubes and nano-silica, Proceedings of the Institution of Mechanical Engineers, Part L: Journal of Materials: Design and Applications, vol. 233, iss. 5, pp. 874-884, doi: 10.1177/1464420717714345
- Qian, M., Song, P., Qin, Z., Yan, S., Zhang, L. (2019). Mechanically robust and abrasion-resistant polymer nanocomposites for potential applications as advanced clearance joints, Composites Part A: Applied Science and Manufacturing, vol. 126, p. 105607, doi: 10.1016/j.compositesa.2019.105607
- Miyoshi, K. (2019). Solid lubrication fundamentals and applications, CRC Press, 2019.
- Ibrahem, R. (2016). Friction and Wear Behaviour of Fibre/Particles Reinforced Polyester Composites, International Journal of Advanced Materials Research, vol. 2, no. 2, pp. 22-26.
- Ibrahim, R. (2016). Influence of natural fillers on tribological and mechanical performance of polyester composites, International Journal of Advanced Materials Research, vol. 2, no. 2, pp. 27-32, 2016,
- Ibrahem, R. A. (2015). Effect of date palm seeds on the tribological behaviour of polyester composites under different testing conditions, Journal of Material Sciences & Engineering, vol. 4, iss. 6, pp. 1-5, 2015, doi: 10.4172/2169-0022.1000206
- Shalwan, A., Yousif, B. F., Alajmi, F. H., Alajmi, M. (2021). Tribological behavior of mild steel under canola biolubricant conditions, Advances in Tribology, vol. 2021, pp. 1-13, 2021, doi: 10.1155/2021/3795831
- Ibrahem, R. A. (2015). Tribological performance of polyester composites reinforced by agricultural wastes, Tribology International, vol. 90, pp. 463–466, 2015, doi: 10.1016/j.triboint.2015.04.042
- Zagho, M. M., Hussein, E. A., and A. A. Elzatahry, A. A. (2018). "Recent overviews in functional polymer composites for biomedical applications," Polymers, vol. 10, no. 7, p. 739, doi: 10.3390/polym10070739.
- Alajmi, A., Abousnina, R., Shalwan, A., Sultan Alajmi, Alipour, G., Tafsirojjaman, T., Will, G. (2022). An Experimental and Numerical Investigation into the Durability of Fibre/Polymer Composites with Synthetic and Natural Fibres, Polymers, vol. 14, iss. 10, 2022, doi: 10.3390/polym14102024
- Darshan S. M., and Suresha, B. (2021). "Effect of basalt fiber hybridization on mechanical properties of silk fiber reinforced epoxy composites," Materials Today: Proceedings, vol. 43, pp. 986–994, Jan. 2021, doi: 10.1016/j.matpr.2020.07.618.
- Darshan, S. M., Suresha, B., and I. M. Jamadar, I. M. (2022). "Optimization of Abrasive Wear Parameters of Halloysite Nanotubes Reinforced Silk/Basalt Hybrid Epoxy Composites using Taguchi Approach," Tribology in Industry, vol. 44, no. 1, pp. 253–267, doi: 10.24874/ti.1131.06.21.08.
- Darshan S. M., and Suresha, B. (2022). "Effect of halloysite nanotubes on Physico-Mechanical Properties of Silk/Basalt fabric reinforced epoxy composites," Materials Science Forum, vol. 1048, pp. 21–32, Jan. 2022, doi: 10.4028/www.scientific.net/msf.1048.21.
- Namdev, A., Telang, A., and R. Purohit, R. (2022). "Experimental investigation on mechanical and wear properties of GNP/Carbon fiber/epoxy hybrid composites," Materials Research Express, vol. 9, no. 2, p. 025303, doi: 10.1088/2053-1591/ac4e3f.
- Vinod, Kumar, A., Suresha, B., Kumar, M., and Ramesh, S. (2018). "Study on Two Body Abrasive Wear behaviour of Carboxyl-Graphene Reinforced Epoxy Nano-composites," IOP Conference Series: Materials Science and Engineering, vol. 376, p. 012058, Jun. 2018, doi: 10.1088/1757-899x/376/1/012058.
- Darshan, S.M., and Suresha, B. (2019). "Mechanical and abrasive wear behaviour of waste silk fiber reinforced epoxy biocomposites using Taguchi method," Materials Science Forum, vol. 969, pp. 787–793, doi:



© 2025. Advanced Journal of Engineering and Scientific Applications (AJESA) Vol. 2, No..1, 2025.

- 10.4028/www.scientific.net/msf.969.787.
- Namdev, A., Purohit, R., and Telang, A. (2023). "Impact of graphene nano particles on tribological behaviour of carbon fibre reinforced composites," Advances in Materials and Processing Technologies, pp. 1–18, Mar. 2023, doi: 10.1080/2374068x.2023.2189670.
- Namdev, A., Telang, A., Purohit, R., and M.K. Agrawal, M. K. (2022). "An experimental assessment of abrasive wear behavior of GNP/Carbon fiber/epoxy hybrid composites," Indian Journal of Engineering and Materials Sciences, vol. 29, no. 6, pp. 777–785, doi: 10.56042/ijems.v29i6.70309.
- Yan, F. (2020). "A novel π bridging method to graft graphene oxide onto carbon fiber for interfacial enhancement of epoxy composites," Composites Science and Technology, vol. 201, p. 108489, Jan. 2021, doi: 10.1016/j.compscitech.2020.108489.
- Chira, A., Kumar, A., Vlach, T., Laiblová, L., Škapin, A. S., and P. Hájek, P. (2016). "Property improvements of alkali resistant glass fibres/epoxy composite with nanosilica for textile reinforced concrete applications," Materials & Design, vol. 89, pp. 146–155, doi: 10.1016/j.matdes.2015.09.122.
- Namdev, A., Telang, A., and Purohit, R. (2021). "Effect of graphene nano platelets on mechanical and physical properties of Carbon Fibre/Epoxy hybrid composites," Advances in Materials and Processing Technologies, vol. 8, no. sup3, pp. 1168–1181, Jun. 2021, doi: 10.1080/2374068x.2021.1939557.
- Shivakumar, H. R., Renukappa, N. M., Shivakumar, K., and B. Suresha, B. (2020). "The reinforcing effect of graphene on the mechanical properties of Carbon-Epoxy composites," Open Journal of Composite Materials, vol. 10, no. 02, pp. 27–44, doi: 10.4236/ojcm.2020.102003.
- Srivastava, A. K., Gupta, V., Yerramalli, C. S., and A. Singh, A. (2019). "Flexural strength enhancement in carbon-fiber epoxy composites through graphene nano-platelets coating on fibers," Composites Part B: Engineering, vol. 179, p. 107539, doi: 10.1016/j.compositesb.2019.107539.
- Kumar, S., Singh, K. K., and Ramkumar, J. (2020). "The effects of graphene nanoplatelets on the tribological performance of glass fiber-reinforced epoxy composites," Proceedings of the Institution of Mechanical Engineers, Part J: Journal of Engineering Tribology, vol. 235, no. 8, pp. 1514–1525, Oct. 2020, doi: 10.1177/1350650120965756.
- Kumar, S., Singh, K. K., and Ramkumar, J. (2020). "Comparative study of the influence of graphene nanoplatelets filler on the mechanical and tribological behavior of glass fabric-reinforced epoxy composites," Polymer Composites, vol. 41, no. 12, pp. 5403–5417, Sep. 2020, doi: 10.1002/pc.25804.
- Scedil, M. C. (2019). "A brief overview on synthesis and applications of graphene and graphene-based nanomaterials," Frontiers of Materials Science, vol. 13, no. 1, pp. 23–32, doi: 10.1007/s11706-019-0452-5.
- Muralidhara, B. K., Babu, S. P. K., Hemanth, G., and B. Suresha, B. (2020). "Optimization of abrasive wear behaviour of halloysite nanotubes filled carbon fabric reinforced epoxy hybrid composites," Surface Topography: Metrology and Properties, vol. 8, no. 4, p. 045028, doi: 10.1088/2051-672x/abc8e1.
- Darshan S. M., and B. Suresha, B. (2019). "Mechanical and abrasive wear behaviour of waste silk fiber reinforced epoxy biocomposites using Taguchi method," Materials Science Forum, vol. 969, pp. 787–793, doi: 10.4028/www.scientific.net/msf.969.787.
- Tahir, N. A. M., Abdollah, M. F. B., Hasan, R., Amiruddin, H. (2016). The effect of sliding distance at different temperatures on the tribological properties of a palm kernel activated carbon–epoxy composite, Tribology International, vol. 94, pp. 352–359, doi: 10.1016/j.triboint.2015.10